

# Chapter 36

## BeiDou Satellite Multipath Characteristics Research-From the “Micro” Parameters Point of View

Xin Chen, Xiaoran Fang, Yuze Wang, Yanhong Kou, Le Cai,  
Peilin Liu and Wenxian Yu

**Abstract** Multipath is one of the most important factors that affect the positioning accuracy of GNSS receivers. Traditionally, the Code-Minus-Carrier Multipath Observable (CMO) is used to study the characteristics of GPS multipath errors, which takes on period fluctuations. However, BeiDou System comprises of three types of satellite—MEO, IGSO and GEO, the orbits of which differ a lot with each other. The standing multipath observed in GEO multipath causes the fluctuation phenomenon obscure, making the research with CMO technique hard to continue. Up till now, only a few literatures focused on studying the characteristics of multipath ‘micro’ parameters like delay, attenuation, carrier phase and number with real-world signal data. Those parameters indeed reflect the behavior of multipath more straightforward. Therefore, the Code Amplitude Delay Lock Loop (CADLL) technique is used at this paper to decompose the multipath at its signal parameter level. The experiment results reveal that even the GEO multipath can also vary slowly because of the satellite perturbation. The GEO multipath fading period can be a few hours. However, the IGSO and the MEO multipath do not show much distinct difference. The specular multipath fading period of both IGSO and MEO is normally a few minutes, while the diffused multipath parameters take on steady behavior but last very short time. It is found as well that the multipath signal of all kinds of satellites bears the nature of limited existing time. Thus, the concept of multipath life-time is proposed in this paper to describe the statistical distribution of

---

X. Chen (✉) · X. Fang · Y. Wang · P. Liu · W. Yu  
Shanghai Key Laboratory of BeiDou Navigation and Location-Based Service,  
School of Electronics, Information and Electrical Engineering,  
Shanghai Jiao Tong University, Shanghai 200240, China  
e-mail: xin.chen@sjtu.edu.cn

Y. Kou  
Department of Electronic and Information Engineering, Beihang University,  
Beijing 100191, China

L. Cai  
Space Star Technology Co., Ltd, Beijing 100086, China

multipath lasting time as well as the multipath power variation feature during its life-time. Those models are useful for simulator design to emulate more precise multipath scenario.

**Keywords** Multipath estimation · CADLL · Life time of multipath · Specular multipath · Diffused multipath

## 36.1 Introduction

Multipath is a major factor that affects the performance of GNSS receiver to be degrading. Since multipath is closely related to application environments, RTK technique cannot remove the positioning errors caused by multipath. Many multipath error mitigation methods have been proposed so far, including choke ring antenna, pseudorange measurement filtering, special code tracking loop design and so on. However, none of them is able to fully resolve the problem. Thus, the research on multipath characteristics of GNSS signal is still an urgent demand.

According to the multipath tap-delay model, a multipath signal can be uniquely expressed by its code phase delay  $\tau$ , amplitude attenuation  $\alpha$  and the changing rate of multipath carrier phase  $\delta f$ .  $\delta f$  is also called multipath error fading frequency since it can caused multipath error to periodically change. At static scenario, multipath error fading frequency depends on the movement of satellite. Literature [1] studied the relationship between multipath error fading and satellite orbits. Traditionally, the Code-Minus-Carrier Multipath Observable (CMO) technique was used to study the features of GPS multipath error [2]. The magnitude of multipath error is able to be measured by manipulating the statistics of CMO [3]. But CMO technique is not so efficient to standing multipath which often appears in WAAS system and SBAS system because the standing multipath error is prone to stay constant. Besides, CMO technique is unable to observe the high frequency part of multipath error [4, 5].

BeiDou system comprises of three types of satellites—GEO, IGSO and MEO, so it has more complex multipath errors. In contrast with CMO, we want to study the multipath characteristics more straightforward from the “micro” parameters point of view, such as multipath delay, power attenuation, carrier phase changing rate, lasting time, etc. Unfortunately, there have only been a few papers so far studying the features of those “micro” parameters of real multipath signal. This is partly due to the complexity of multipath parameter estimation algorithm. But some research entities have designed their multipath estimation methods and been studying the multipath channel of GPS [6].

The authors of this paper proposed a multipath estimation and mitigation algorithm named Coupled Amplitude and Delay Lock Loops (CADLL) in 2011. It is able to detect and estimate multipath with intermediate frequency (IF) sampling data. The parameters of those detected will be continuously tracked and recorded.

In this paper, we used the GNSS Application-defined Software Receiver-multipath mining (GSAR-mm) to process the IF data sampled at two multipath spots, and present the multipath features and models that was found during these experiments.

### 36.2 Multipath Mathematic Model

#### 36.2.1 Multipath Signal Mathematic Expression

A multipath ray can be uniquely determined by its code phase delay  $\tau$ , power attenuation  $\alpha^2$ , carrier phase  $\varphi$  and the carrier phase changing rate  $\delta f = d\varphi/dt$ . All those parameters are measured with respect to direct line-of-sight signal (DLOS). Those signal rays that go into the antenna at multipath scenario are expressed as:

$$s(t) = AD(t) \sum_{n=0}^M \alpha_n c(t - \tau_n) \cos(2\pi ft + \varphi_n) \tag{36.1}$$

where  $A$  is the DLOS amplitude,  $D(t)$  is the navigation bit,  $c(t - \tau_n)$  is the spreading code.  $n = 0$  means the DLOS. By default, DLOS has  $\alpha_0 = 1$ ,  $\tau_0 = 0$ ,  $\varphi_0 = 0$ . The multipath error fading frequency  $\delta f$  is due to the change of delay caused by the relative movement between satellite and receiver. The relationship of multipath, DLOS and the composite signal can be illustrated by the phasor diagram (Fig. 36.1).

The positive multipath ( $|\varphi_n| \leq 90^\circ$ ) will increase the composite signal's power, but the negative multipath ( $|\varphi_n| > 90^\circ$ ) will reduce the composite signal's power. Both of them can affect the accuracy of pseudorange measurement, thus leading to positioning errors.

#### 36.2.2 Multipath Signal Propagation Geometric Model

There are mainly two types of multipath: specular multipath and scattering multipath. Specular multipath is normally produced by the reflection of DLOS on a plain,

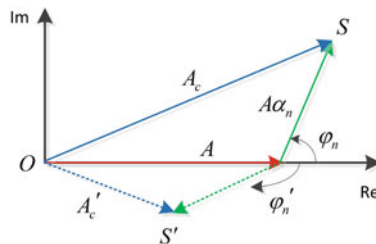
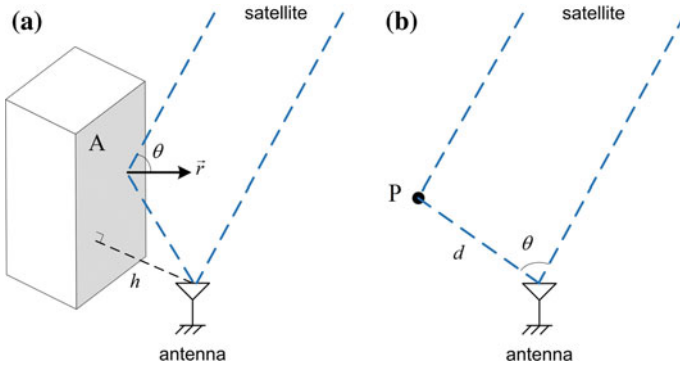


Fig. 36.1 The phasor diagram of multipath signal and DLOS signal



**Fig. 36.2** Multipath propagation geometric model. **a** Specular multipath model. **b** Scattering multipath model

which follows the mirror reflection law. Scattering multipath occurs when the DLOS goes incident into an irregular scattering point or the intersection line of two plains. This kind of multipath can be modeled as propagating at a certain direction angle from the scattering point. The propagation models of both specular and scattering multipath are shown in Fig. 36.2:

In Fig. 36.2a,  $A$  is the reflection plane;  $h$  is the perpendicular distance from antenna to plane  $A$ ;  $\vec{r}$  is the normal vector of plane  $A$ ;  $\theta$  is the reflection angle. The multipath delay of specular geometric model is:

$$L_{\text{specular}} = 2h \cos \theta \quad (36.2)$$

In Fig. 36.2b,  $P$  is the scattering point;  $d$  is the distance from antenna to  $P$ ;  $\theta$  is the included angle between multipath and DLOS. The delay of scattering mode is:

$$L_{\text{scatter}} = d(1 - \cos \theta) \quad (36.3)$$

If we denote the carrier wavelength as  $\lambda$ , the multipath carrier phase can be deduced from the delay:

$$\varphi_n = 2\pi L/\lambda + \Delta\varphi \quad (36.4)$$

where  $\Delta\varphi$  is the phase abrupt change induced by reflection or scattering.  $\Delta\varphi$  is normally constant as long as the material property of the reflection plane or scattering point does not change.

At static scenario, the movement of satellite will cause the change of multipath delay, then leading to the change of multipath carrier phase. Therefore, the multipath error fading frequency can be computed from the derivative of phase:

$$\delta f_n = d\varphi_n/dt/2\pi = dL/dt/\lambda \quad (36.5)$$

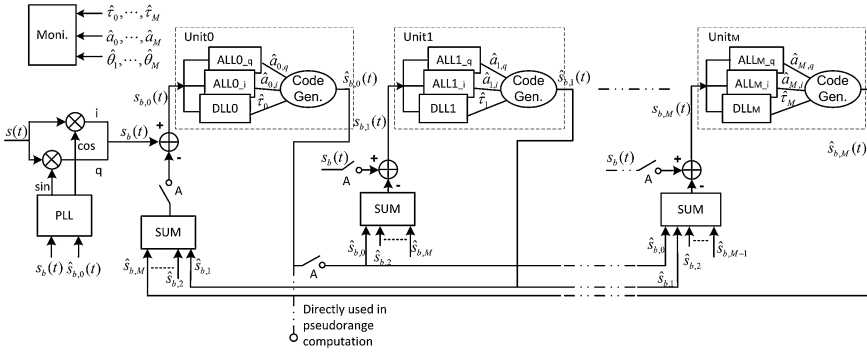


Fig. 36.3 Block structure of CADLL

### 36.2.3 Coupled Amplitude and Delay Lock Loops

The structure diagram of CADLL algorithm is shown in Fig. 36.3. It is able to detect and estimate multipath with IF sampling data. This architecture exploits the “turbo principle” to separately track the Line Of Sight (LOS) signal and multipath signals in order to mitigate the effects of the multiple reflections. The Delay Lock Loop (DLL) and the Amplitude Lock Loop (ALL) are two basic elements in the structure. DLL is in charge of estimating and tracking the code delay of a specific ray in the incoming signal while ALL is in charge of estimating the corresponding amplitude. A pair of DLL and ALL makes a Unit, devoted to track LOS or a multipath signal. Several Units are incorporated in the CADLL structure, and then able to track the different component rays from the overall incoming signal. The feedback architecture and special working strategy of CADLL boost the performances of the parameter estimation accuracy.

The working procedure of CADLL is also very important. It first uses a conventional tracking loop to lock onto the incoming signal, getting a rough estimation about position of LOS’ code phase; then it activates two units to try to track a multipath signal. If it fails, it means there is no multipath in the incoming signal; if it succeeds, it will continue trying to insert a new unit into this feedback loop to look for a new multipath component. The monitor block is governing the process of searching a new multipath component by checking the tracking results of the new unit. If it is considered that there is no new multipath component, the trial unit will be shut down by the monitor block. The process will not stop until there is no new multipath found or the number of enabled units reaches the maximum number  $M_M$ , which is pre-defined according to available resources. Following this specially designed working procedure, CADLL actually has the ability of estimating the number of multipaths and adjusting its structure to match it. The detailed introduction and performance about CADLL can be found in [7, 8].

We used the GNSS signal analyzing receiver GSARx-mm to process the real signals sampled at two representative multipath spots. One is at Shanghai Jiao Tong University (SJTU) and the other is at Beijing Beihang University. The results are shown in the next section.

## 36.3 Multipath Signal Analyzing Campaign


### 36.3.1 SJTU Multipath Data Processing Results

The first experiment place is at the patio of Weidianzi Building of SJTU Minghang campus. Two pieces of IF data were sampled at two different time. The specification about the sampling device and the field picture are listed in Table 36.1.

By processing SJTU data1, a multipath was clearly found in the BDS GEO4 signal. This multipath existed about 6805 s in this data. Its delay was about 24.6 m and the carrier phase was mostly staying at  $-150^\circ$ , which means a typical standing multipath. However, its power attenuation kept increasing, from the initial  $-8$  dB to the final  $-16$  dB. This explains why the variances of multipath delay and carrier phase estimations kept increasing. The estimation results of the delay, carrier phase, power attenuation and the correlation shapes are shown in Fig. 36.4. From the correlation shape figure, it can be seen that the original signal's correlation shape, which is denoted by the black line was distorted by multipath, while the correlation shape of the restored DLOS signal shows a good symmetry.

In order to figure out how and where the multipath in BDS GEO4 was generated, we surveyed the surrounding buildings of the antenna by using Huace company's high-performance receiver model N71 which can give centimeter level positioning results. The surveyed points for determining the plains of the surrounding buildings are those on the roof of the buildings and with open view of sky, so no multipath interference is in there. In order to determine the plane of the patio, we chose the points at the southeast edge of the patio where is far from other reflection planes and we also checked the signals with GSARx-mm and excluded the possible multipath interference. When all the geometric models about the experiment environment are

**Table 36.1** Experiment situations at SJTU

Place	At the patio of Weidianzi Building, SJTU Minghang campus	Time	Data 1: sampled at 3:00 p.m. on Nov. 15th 2014, length of about 2 h
			Data 2: sampled at 21:36 on Nov. 25th 2014, length of about 1 h and 6 min
Sampling parameters	Sampling freq.: 62 MHz	Field picture	
	RF bandwidth: 40 MHz		
	Quantization: 8 bit		
	Sampling mode: Complex sample		

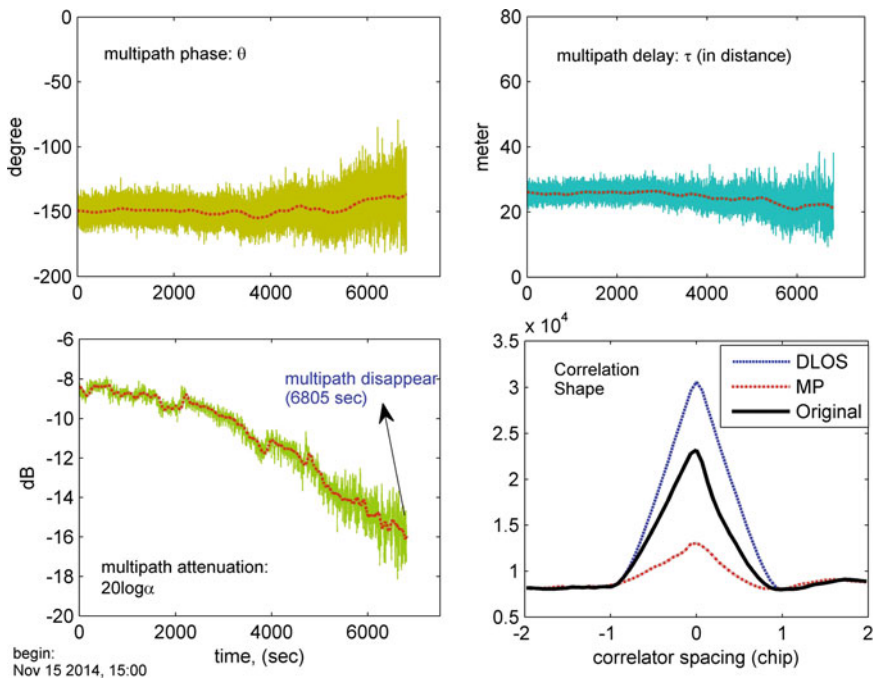


**Fig. 36.4** BDS GEO4 B1 multipath signal’s phase degree, delay, attenuation and correlation shape of SJTU data1

established, the geodetic coordinates of the antenna is also able to be obtained by measuring the distance from the antenna point to all other surveyed points. The surveyed geodetic coordinates of the antenna is (31.0250N, 121.4396E, 23.7953H).

It is needed to clarify that although the receiver N71 can give us centimeter level accuracy when determining the relative geometric models of the buildings, the geodetic coordinates of those surveyed points can have consistent biases of even a few meters. This is because the CORS networks we used is not so reliable (built by Huace company itself) and the baseline is comparatively far (>30 km). But these errors will not cause any significant effects on our experiments.

By combining the antenna coordinates, surrounding buildings’ geometric models and the GEO4 satellite orbit information, we constructed a local level coordinate system with the antenna as the origin and computed the possible multipath reflection paths. The results are shown in Fig. 36.5. It is found that Plane N2 does not meet the reflection condition for GEO4 signal. The delays produced by the reflection path of Plane N1 and the reflection path of Plane W1 are 11 and 3.96 m respectively, which is quite different from the estimated delay (24.6 m) shown in Fig. 36.4. It can be concluded that the multipath detected in the data1 is not produced by those one-reflection paths.

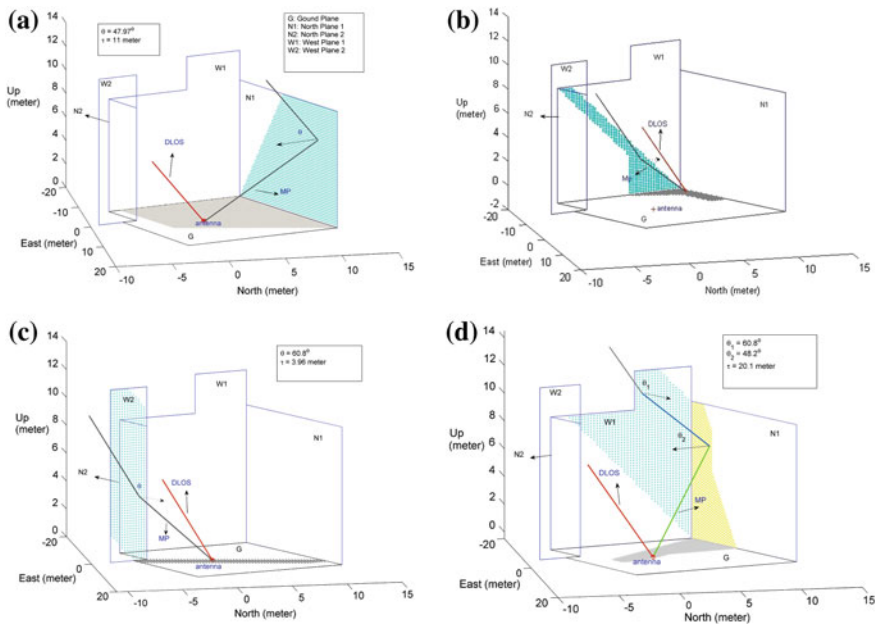


**Fig. 36.5** Theoretical reflection paths by the surrounding buildings. **a** Possible reflection path by North1 plane. **b** Possible reflection path by West1 plane. **c** Possible reflection path by West2 plane. **d** Possible double reflection path by West1 and North1 planes

Figure 36.5d shows a double-reflection multipath model, firstly by Plane W1 and then by Plane N1. The delay produced by this path is about 20.1 m. Considering the estimation noise effects and the surveyed errors of the buildings, it can be deduced that this double-reflection model is consistent with the detected one in the experiment. This experiment tells us that under complex multipath scenario the power of one-reflection multipath is even weaker than that of double-reflection multipath. The polarization of one-reflection multipath is normally left-handed, whereas the double-reflection multipath is changed back to right-handed polarization, so this change makes the selectivity of GNSS antenna invalid for it.


The processing results of SJTU data2 are shown in Fig. 36.6. It is found that there is a multipath in MEO12 signal, whose delay is about 25 m. Because of the movement of MEO satellite, the delay takes on an incremental trend. The curve fitting result for the multipath carrier phase shows that its multipath carrier phase change rate is approximately 0.00264 Hz (6.31 min/cycle). So the delay increases by about 6.2 wavelengths during the entire data time length. It is also noted that there are interruptions of the tracking onto this multipath. It is because the materials of the reflection plane are not homogeneous, so it will cause reflection power fading during the satellite’s movement. This phenomenon also appears in the Beihang university experiment data (Table 36.2).



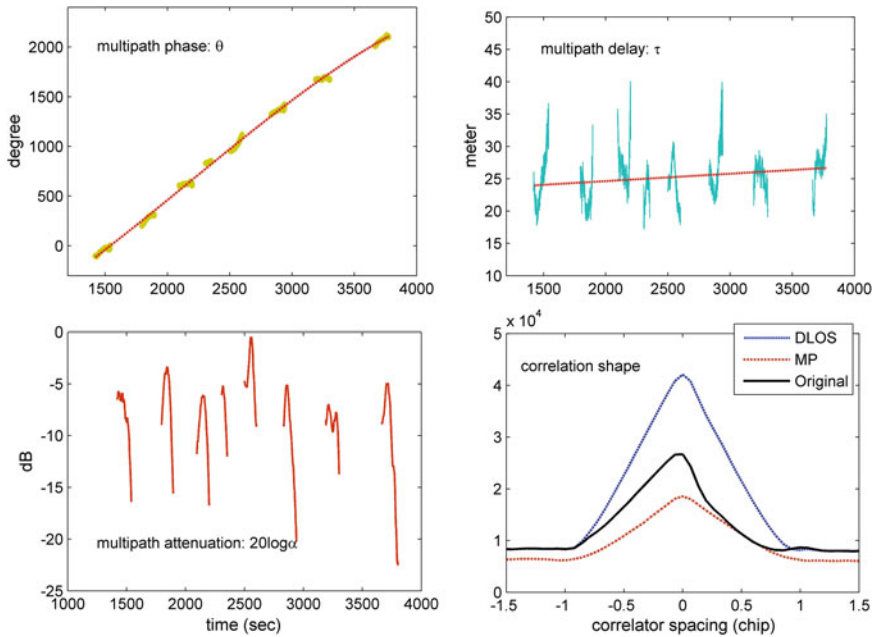


**Fig. 36.6** BDS MEO12 B1 multipath signal’s phase degree, delay, attenuation and correlation shape of SJTU data 2

**Table 36.2** Experiment situations at Beihang University

Place	On the roof of New Building F Section of Beihang University Campus	Time	Sampled at 9:03 a.m. on Sept. 3rd 2014, length of about 1 h and 20 min
Sampling parameters	Sampling freq.: 100 MHz	Field picture	
	RF bandwidth: 40 MHz		
	Quantization: 12 bit		
	Sampling mode: RF sampling		

### 36.3.2 Beihang Multipath Data Processing Results

By processing Beihang data, we found that there are multipaths in both GEO5 and IGSO10 signals. Figure 36.7 illustrates the parameter estimation results of the GEO5 multipath. Its delay is about 81 m and has a decreasing trend. Because of the permutation of GEO satellite, the multipath still has a minor fading frequency of  $-4.083e-5$  Hz (6.8 h/cycle). Because we did not get the surveyed information about this experiment environment, we could not build the corresponding multipath geometric model, but it is able to speculate from the field picture that the multipath might be produced by the nearby glass wall.

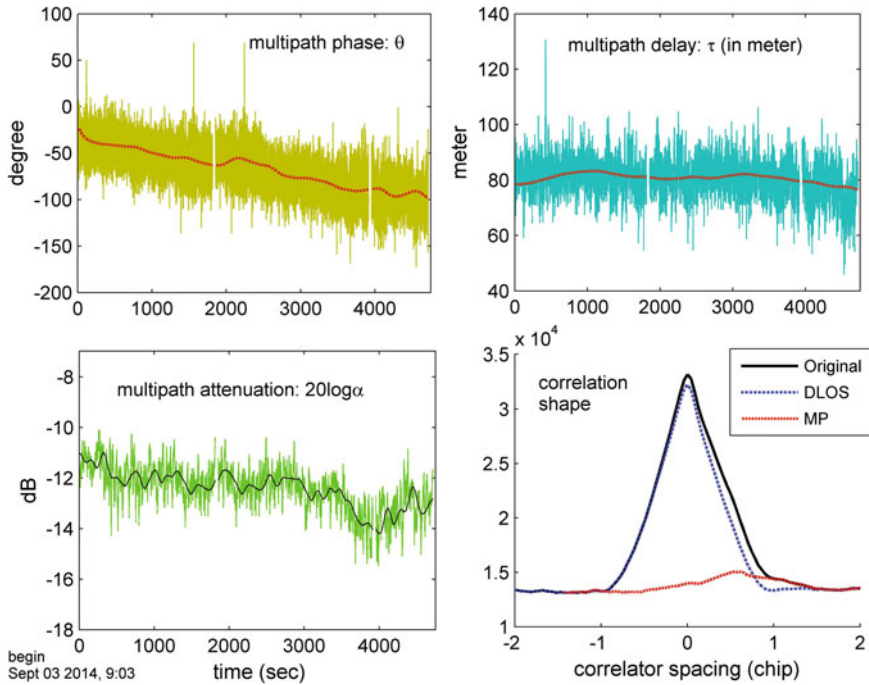


**Fig. 36.7** BDS GEO5 B1 multipath signal’s phase degree, delay, attenuation and correlation shape of Beihang data

Apart from GEO5, IGSO10 is detected to have several multipath signals as well. During 0–180 s, there exist tens of detectable multipath pieces, which belong to three groups of reflection sources. Among all the multipath signals in Fig. 36.8, the red one lasts more than 1500 s and its delay is about 85 m. Its carrier phase and delay curve fitting results prove that these detected pieces belong to one multipath signal, but the power attenuation fluctuation causes the tracking interruptions. The fading frequency is  $-0.0078$  Hz (2.14 min/cycle). The green one’s and the yellow one’s delays are about 40.5 and 25 m respectively. They have comparatively short delays, slow multipath fading, and short lasting time, so it can be speculated that they are produced by the nearby small dimensional specular reflection/scattering sources.

In Fig. 36.8, we find the discontinuous multipath tracking phenomenon again. It is caused by the heterogeneous material of the reflection plane. Take the Beihang experiment spot as an example, the reflection plane is composed of glass and coarse bricks. When the satellite is moving, the reflection point for the same multipath is actually moving on the plane as well, according to the multipath propagation model in Fig. 36.2. Therefore, if the reflection point is on the glass wall, the reflection power is strong and it is easier for the software to detect the multipath. However when the reflection point moved to the brick wall, scattering might happen and the attenuation is increased, so it might be too weak for the software to track the multipath.

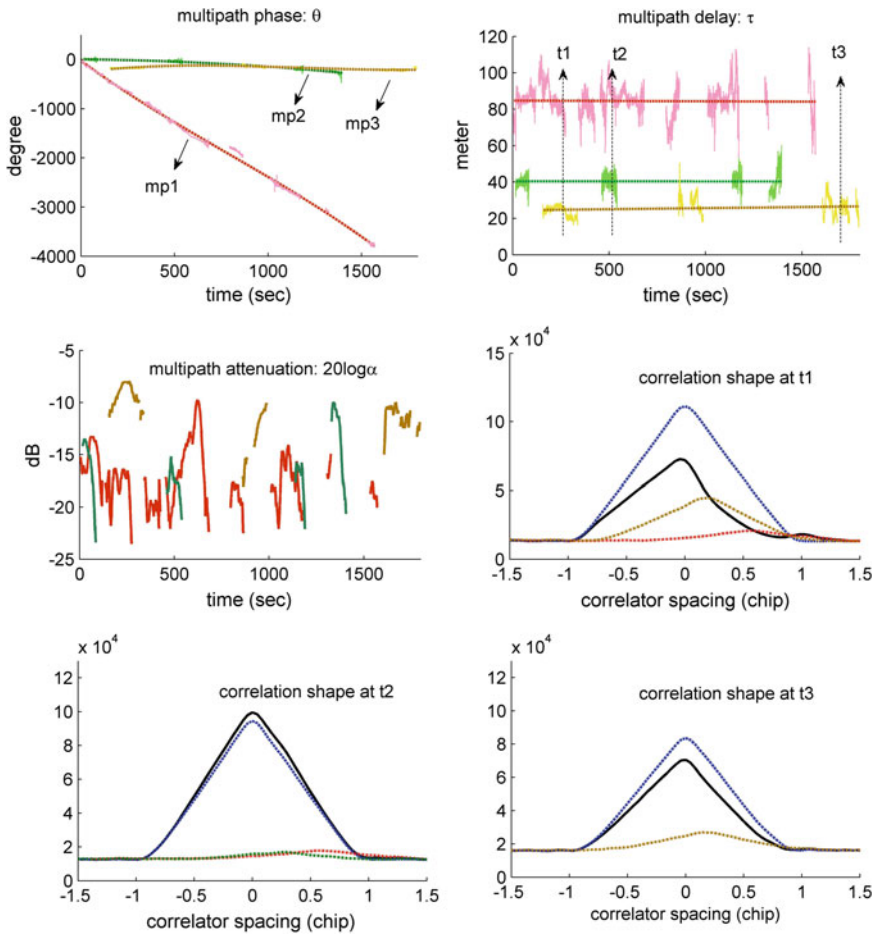


**Fig. 36.8** BDS IGSO10 B1 multipath signals' phase degrees, delays, attenuations and correlation shapes of Beihang data

### 36.3.3 Some Conclusions from the Experiments

Some rules about BDS multipath can be drawn from the above experiment results:

- (1) The perturbation of GEO satellite can make its multipath parameter slowly change as well, even if the antenna is at static. GEO multipath carrier fading period is within a few hours to tens of hours.
- (2) IGSO and MEO multipath exhibits fast carrier phase fading frequency. The fading period is within a few minutes to tens of minutes.
- (3) At complex multipath scenario, the multipath might experience more than once reflection before entering antenna (like the case in Fig. 36.4). Normally

the multipath experiencing one reflection has left-handed polarization, and the one with twice reflections has right-handed polarization again. As a result, such kind of multipath is able to cause much larger errors.

- (4) All kinds of multipath have the feature of limited life time which means that none multipath can last forever even if for GEO. Both the limited dimension of the reflection/scattering source and the movement or perturbation of the satellites could cause the power of multipath decrease or even disappear, making any multipath signal with limited life time. The GEO multipath has the longest life time, normally a few hours. The specular multipath of IGSO and MEO has a life time of tens of minutes to 1 h. The scattering multipath of IGSO and MEO has the shortest life time, often tens of seconds.
- (5) For IGSO or MEO multipath, there might happen multipath tracking interruptions even if during their life time period. This is caused by the heterogeneous property of the reflection material.

### 36.4 Multipath Life-Time Probability Distribution Model

Since multipath signal is closely related to the surrounding environment, the characteristics of those “micro” parameters of multipath are often described by some probability distribution models. According to the research results in [9], the delay of multipath  $\tau$  follows an exponential distribution:

$$f(\tau) = \frac{1}{\tau_0} e^{-\frac{\tau}{\tau_0}} \quad (36.6)$$

The multipath power attenuation  $\alpha^2$  follows an exponential function with the delay  $\tau$  as variable.

$$S(\tau) = S_0 e^{-\delta\tau} \quad (36.7)$$

where  $\tau_0$  is the decay factor in the delay model,  $\delta$  is the decay factor in the power attenuation model, and  $S_0$  is the average multipath attenuation with respect to scenario.

However, none of papers have clearly described the life-time concept about multipath signal so far. At this paper, we propose the multipath life-time parameter which will express the time for a multipath from emerging to extinction. Table 36.3 lists the existing time of all multipath signals detected in the above experiments.

It can be seen from Table 36.3 that at static scenario, the life time of GEO multipath is often greater than 1 h; the life time of IGSO/MEO specular multipath is normally within 1 h; while that of IGSO/MEO scattering multipath is often lying

**Table 36.3** Multipath life-time

No	Satellite type	Multipath type	Life-time (s)	Multipath fading frequency (Hz)
1	GEO	Specular	>6800	<1.389e-5
2	GEO	Specular	>4710	-4.083e-5
3	IGSO	Specular	1570	-0.0078
4 <sup>a</sup>	IGSO	Specular	1150	-0.0056
5 <sup>a</sup>	IGSO	Specular	900	-0.0097
6	IGSO	Scattering	180	<1.528e-4
7	IGSO	Scattering	25	-0.005
8	IGSO	Scattering	70	-0.00283
9	IGSO	Scattering	180	<2.78e-6
10	IGSO	Scattering	55	4.028e-4
11 <sup>a</sup>	IGSO	Scattering	75	<3.472e-4
12	MEO	Specular	2360	0.00264

<sup>a</sup> Stands for those multipaths without plotted at this paper

between 30 s and 5 min. We construct a modified Gamma probability distribution model to describe the life time of different multipaths:

$$T_{mp} - d \sim Gamma(a, b) = \frac{(T_{mp} - d)^{a-1} e^{-\frac{T_{mp}-d}{b}}}{b^a \Gamma(a)} \tag{36.8}$$

where  $a$  is the shape factor,  $b$  is the scale factor, and  $d$  is the offset factor. Figure 36.9 shows the three kinds of multipath life time distributions with Gamma functions. In Fig. 36.9 the life time of GEO multipath is in units of hour, expressed at the bottom axis; while the life time of IGSO and MEO multipath is in units of minutes expressed at the top axis.

It can be observed from the experiments that multipath power will decrease at the end of its life time. This trend will continue until it is deemed as disappeared. Regarding to this property we construct a logarithm function to model the power variation behavior:

$$S(t)|_{dB} = S(\tau)|_{dB} - 5 \log \left( 1 + \varepsilon^2 \left( \frac{t}{T_{mp}} \right)^{2n} \right) \tag{36.9}$$

where  $S(\tau)$  is the multipath power attenuation obtained from Eq. (36.7),  $T_{mp}$  is the multipath life time obtained from Eq. (36.8),  $\varepsilon$  and  $n$  are the model parameters related to the types of multipath.

Figure 36.10 shows the comparisons between the estimated multipath power attenuations from the data and the model curves from Eq. (36.9) of four representative multipaths selected from Table 36.3. Multipath No1 and No2 are GEO's. They take on slow changing behavior because of the slow movement of GEO satellites. Multipath No12 and No11 are the MEO specular multipath and the IGSO

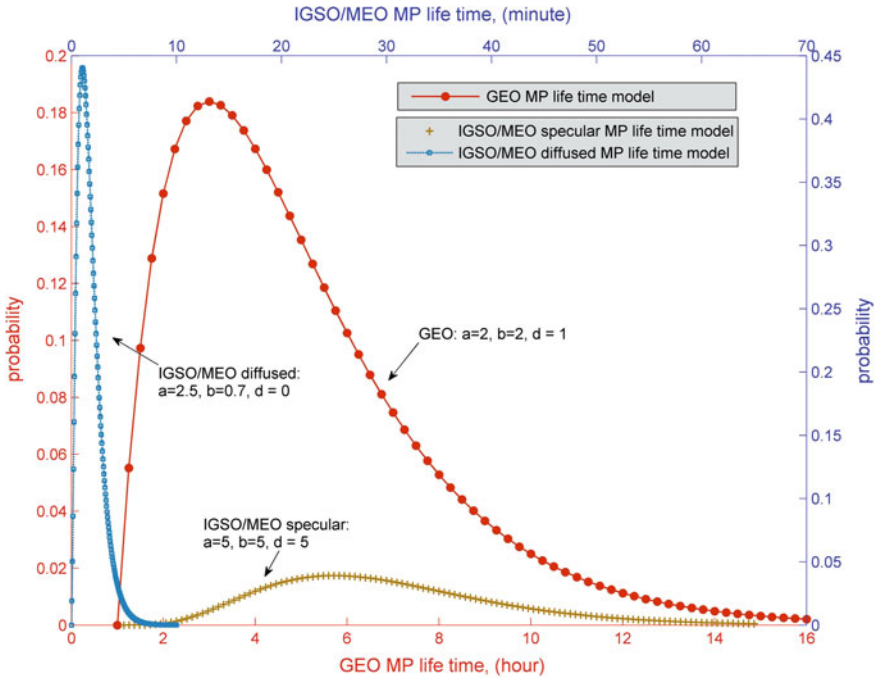


Fig. 36.9 GEO/IGSO/MEO multipath life-time probability distribution models

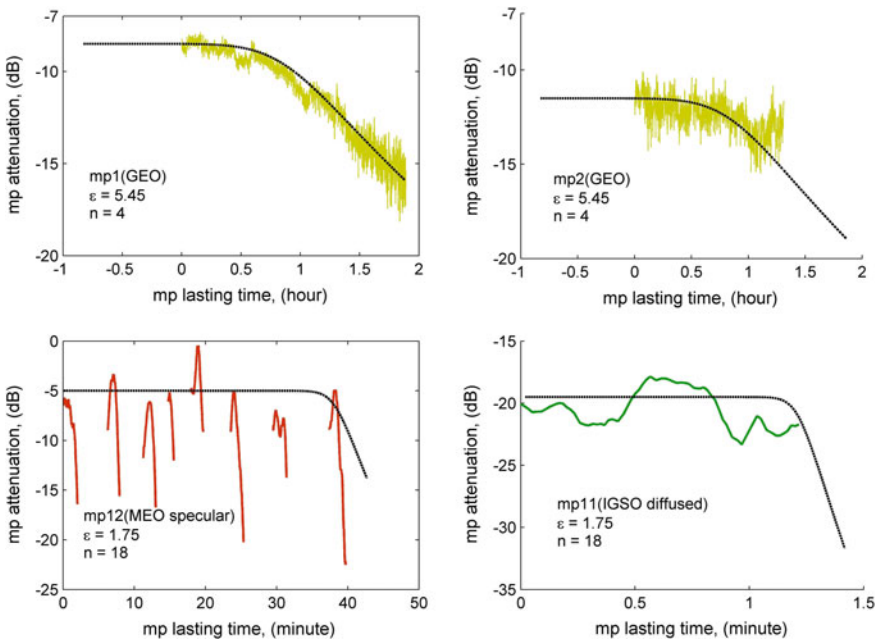


Fig. 36.10 Multipath attenuation evolution in its life time

scattering multipath respectively. So their power curves have much faster decreasing at the end of life time. Comparing the specular multipath and scattering multipath, we can also find that the scattering one have much larger attenuation than the specular reflection one.

Equations (36.6)–(36.9) can be used to design static multipath scenarios for GNSS simulators. It can help the developers to know how the tested receivers will perform under real applications. However, those models proposed at this paper are still needed to be improved because the limited number of multipath samples obtained from the experiments prevents getting more reliable model parameters. Besides, we also need to have more experiments to model the tracking interruption behaviors for the IGSO/MEO specular multipath.

## 36.5 Conclusions

In this paper, two real multipath signal experiments and analyzing campaigns were conducted respectively at Shanghai and Beijing. Multipaths are observed in GEO, IGSO and MEO signals and include both specular reflection multipath and scattering multipath. By extracting the “micro” parameters, it is found that apart from the delay, attenuation and carrier phase change, multipath also has the property of life time and time-variant power attenuation.

Because of the perturbations, the parameters of GEO multipath have very slowly time-variant changing behavior. Whereas there is not much characteristic difference between IGSO multipath and MEO multipath although these two kinds of satellite are quite different in orbits. Specular reflection multipath and scattering multipath show much distinct difference in power attenuation, carrier phase changing rate and life time. Scattering multipath has more attenuation, shorter life time and slower carrier phase changing rate. In the experiments, the multipath with double reflections is also observed. This kind of multipath has even more effects on receiver because their polarization might become right-handed again.

The multipath life time probability distribution model is proposed in this paper to model the statistical property of multipath existing time. Besides, the time-variant power attenuation function is built to precisely model the multipath power change during its life time. These models will be helpful for the GNSS simulator designs.

The future work about this research will focus on more extensive multipath scenarios’ data analyzing to build more accurate models. And the dynamic multipath channel at urban areas will also be studied.

**Acknowledgments** The research work is funded by National Natural Science Foundation of China (No. 61304225); by the Open Research Fund of The Academy of Satellite Application (grant No. 2014\_CXJJ-DH\_04); by the Science and Technology Commission of Shanghai Municipality (grand No. 13511501302).

## References

1. Yang G, Cui X, Lu M, Li H, Feng Z (2012) The analysis and simulation of multipath error fading characterization in different satellite orbits. In: China satellite navigation conference (CSNC) 2012 proceedings, Guangzhou, China, 15–19 May
2. Misra P, Enge P (2006) Global positioning system—signals, measurements, and performance, 2nd edn. Ganga-Jamuna Press, Lincoln
3. Akos DM, Weiss JP, Murphy T, Pullen S (2004) Airborne multipath investigation via a GPS software receiver. In: Proceedings of ION GPS/GNSS 2004, Long Beach, CA, 21–24 Sept
4. Schempp T (2008) WASS benefits of GEO ranging. In: Proceedings of ION GNSS 2008, Savannah, GA, 16–18 Sept
5. Wanninger L, Wallstab-Freitag S (2007) Combined processing of GPS, GLONASS, and SBAS code phase and carrier phase measurements. In: Proceedings of ION GNSS 2007, Fort Worth, TX, 25–28 Sept
6. Xie P, Petovello MG (2011) Multipath signal assessment in the high sensitivity receivers for vehicular applications. In: ION ITM 2011, Portland OR, USA, 19–23 Sept
7. Chen X, Dovis F, Peng S, Morton Y (2013) Comparative studies of GPS multipath mitigation methods performance. *IEEE Trans Aerosp Electron Syst* 39(3):1555–1568
8. Chen X, Dovis F, Pini M, Mulassano P (2011) Turbo architecture for multipath mitigation in global navigation satellite system receivers. *J IET Radar Sonar Navig* 5:517–527
9. Jahn A, Bischl H, Hein G (1996) Channel characterisation for spread spectrum satellite communications. In: *IEEE 4th international symposium on spread spectrum techniques and applications*, Mainz, Germany, vol 3, pp 1221–1226, 22–25 Sept